

Are your **MRI contrast agents** cost-effective?

Learn more about generic **Gadolinium-Based Contrast Agents**.



**FRESENIUS  
KABI**

caring for life

**AJNR**

**Creutzfeldt-Jakob Disease Involvement of  
Rolandic Cortex: A Quantitative Apparent  
Diffusion Coefficient Evaluation**

Y.-R. Lin, G.S. Young, N.-K. Chen, W.P. Dillon and S.  
Wong

This information is current as  
of April 16, 2024.

*AJNR Am J Neuroradiol* 2006, 27 (8) 1755-1759  
<http://www.ajnr.org/content/27/8/1755>

Y.-R. Lin  
G.S. Young  
N.-K. Chen  
W.P. Dillon  
S. Wong

# Creutzfeldt-Jakob Disease Involvement of Rolandic Cortex: A Quantitative Apparent Diffusion Coefficient Evaluation

**BACKGROUND:** Previous reports have suggested that abnormally reduced water diffusivity and T2 prolongation involving cerebral gray matter in patients with early sporadic Creutzfeldt-Jakob disease (sCJD) involves all areas of neocortex with similar frequency, except for primary sensorimotor cortex (Rolandic cortex) and visual cortex. Rolandic cortex often appears to be spared even in the presence of extensive surrounding neocortical signal intensity abnormality in adjacent frontal and parietal gray matter. A quantitative apparent diffusion coefficient (ADC) analysis was designed to investigate whether this unusual pattern results from pathophysiologic sparing of Rolandic cortex or from reduced conspicuity of signal intensity abnormality on MR imaging echo-planar diffusion-weighted images (epiDWI) related to unknown underlying features of Rolandic cortex.

**METHODS:** ADC maps were derived from epiDWI of 6 patients with sCJD and 8 control patients. Bilateral regions of interest were manually selected in precentral gyri, superior frontal gyri, postcentral gyri, supramarginal gyri, thalamus, putamen, and caudate nuclei. ADC and relative ADC (rADC) values were calculated for each region of interest.

**RESULTS:** Patients with CJD had significantly lower ADC values than control patients in all areas ( $P \leq 0.05$ ). The trend toward decreased ADC values in the deep nuclei correlates well with previously published reports. rADC were not significantly different between CJD and control groups in any area ( $P > 0.25$  in all cases).

**CONCLUSION:** Quantitative ADC measurements in patients with early sCJD demonstrate a similar degree of reduced water diffusivity in the primary somatosensory cortex as in other neocortical areas, despite the normal appearance of these areas on visual inspection of epiDWI.

The characteristic manifestations of sporadic Creutzfeldt-Jakob disease (sCJD) on echo-planar diffusion-weighted MR imaging (epiDWI) and T2-weighted fluid-attenuated inversion recovery imaging (FLAIR) have been well described in a number of recent articles and include the reduction of water diffusivity and prolongation of T2 relaxation time (T2) within the cerebral cortex and deep gray matter (GM).<sup>1,2</sup> Strong correlation between regional distribution of spongiform degeneration at autopsy and abnormal water diffusivity on epiDWI in 2 patients suggests that abnormal water diffusivity is closely correlated with prion-related neuronal injury, at least in late CJD.<sup>3</sup> Recent analyses have demonstrated very high sensitivity and specificity (>90%) for CJD diagnosis using epiDWI combined with FLAIR imaging.<sup>4-6</sup>

Qualitative analysis of the distribution of abnormality on epiDWI and FLAIR in a recently published early sCJD MR imaging study showing >90% sensitivity overall, revealed abnormal T2 prolongation and reduced diffusivity occurring with similar frequency in all areas of neocortex except the pri-

mary sensorimotor cortex ("Rolandic cortex") and visual cortex. Surprisingly, Rolandic cortex signal intensity on FLAIR and epiDWI appeared normal in all 40 patients in this series, even in the presence of extensive abnormality in adjacent frontal and parietal GM.<sup>6</sup> This apparent "Rolandic cortex sparing" seems unusual for a disease with protean clinical manifestations and a systemic etiology, and although histopathologic examination of Rolandic cortex is impossible in early CJD, autopsy brain specimens show severe neuronal loss, spongiosis, and gliosis in the central gyrus.<sup>7</sup> Thus we hypothesized that in early prion parenchymal injury, an unknown feature intrinsic to Rolandic cortex may conceal reduced diffusivity in this cortical area from discovery by qualitative (visual) inspection of epiDWI. Because apparent diffusion coefficient (ADC) mapping allows analysis of altered water diffusivity independent of the underlying abnormal T2 prolongation or shortening that affects the signal intensity of epiDWI, we designed a quantitative ADC analysis of a subset of the previously reported cohort to determine whether visually undetectable abnormal diffusivity exists in Rolandic cortex.

## Methods

### Subjects

Six patients with CJD (1 man, 5 women) from the previously reported cohort for whom digital data were available<sup>6</sup> were included in this study. The CJD group included 5 patients with definite sCJD and 1 patient with definite familial CJD (fCJD). Two examinations were available from 1 of the sCJD patients. Digital epiDWI data from 8 control patients with nonprion dementias, from the same previously reported cohort, were also analyzed (4 men, 4 women). The control group included patients with diagnoses of Alzheimer disease, mild

Received October 3, 2005; accepted after revision December 7.

From the Department of Radiology (Y.-R.L., G.S.Y., N.-K.C., S.W.), Brigham and Women's Hospital-Harvard Medical School, Boston, Mass; HCNR Center for Bioinformatics (Y.-R.L.), Harvard Medical School, Boston, Mass; Department of Electronic Engineering (Y.-R.L.), National Taiwan University of Science and Technology, Taipei, Taiwan, R.O.C.; and Department of Radiology (W.P.D.), University of California at San Francisco, San Francisco, Calif.

Y.-R.L. and G.S.Y. contributed equally to this work.

Presented at the Annual Meeting of the Radiological Society of North America; Nov 27-Dec 2, 2005; Chicago, Ill.

Address correspondence to Geoffrey S. Young, MD, Instructor in Neuroradiology, Department of Radiology, Brigham and Women's Hospital, 75 Francis St, Boston MA 02115; e-mail: gsyong@partners.org

cognitive impairment, progressive supranuclear palsy, corticobasal degeneration, dementia unspecified (nonprion), and clinically normal. The age ranges of the control patients ( $66.1 \pm 14.9$  years) and CJD patients ( $63 \pm 8.3$  years) were similar.

Prior approval was obtained from the Institutional Review Boards at the participating institutions for acquisition and retrospective analysis of data.

### Image Acquisition

All MR examinations were performed on a 1.5T MR system with  $>20$  mT/m fast gradients and echo-planar imaging (EPI) capability, using a single-channel, circularly polarized head coil. The details of diagnostic MR imaging (FLAIR) scan parameters have been reported previously.<sup>6</sup>

### Diffusion Weighted Imaging

Whole-brain, axial-plane epiDWI were acquired using a spin-echo, echo-planar imaging sequence. The diffusion-sensitizing gradients were applied along 3 directions: section selection, phase encoding, and readout with the diffusion weighting factor  $b = 1000$  s/mm<sup>2</sup>, plus 1 reference scan with  $b = 0$ . Scan parameters included acquisition matrix size,  $128 \times 128$  (interpolated to  $256 \times 256$  for display), field of view, 24–36 cm; section thickness, 5 mm (no intersection gap); repetition time (TR), 8000–10,000 ms; and echo time (TE), 97.4–113.7 ms.

### Data Analysis

The acquired images were analyzed with a software package developed in house, based on the Matlab (MathWorks, Natick, Mass) platform running on a personal computer. The equation published by Stejskal and Tanner<sup>8</sup> was used for ADC calculation:  $ADC = -\{\ln(S1/S2)/(b1 - b2)\}$ , where S1 and S2 are the signal intensities of diffusion-weighted images with applied b-factors 1 ( $b1$ ) and 2 ( $b2$ ), respectively. The ADC maps were computed on a voxel-by-voxel basis by averaging the ADCs calculated from the 3 orthogonal directions.

Regions of interest (ROI) were manually selected to encircle the cortex of the selected gyri while excluding the adjacent CSF and subcortical white matter (WM). All ROIs were reviewed by a neuroradiologist blind to diagnosis, before data analysis. ROIs were traced on EPI T2-weighted images (ie, the  $b = 0$  epiDWI) acquired as part of the epiDWI sequence. These images are acquired in the same coordinate space as the  $b = 1000$  epiDWI but provide superior contrast between CSF and cortex compared with the  $b = 1000$  epiDWI images. The EPI T2-weighted image data were chosen for ROI selection, instead of other structural MR imaging data, to avoid any potential for misregistration related to patient motion and inconsistent geometric distortions between EPI and non-EPI sequence MR imaging. To reduce possible errors related to the partial volume effect of subcortical WM on normal appearing T2-weighted images, visual ROI prescription was constrained with an algorithm that incorporated prior anatomic knowledge of the thickness of neocortex. Voxels prescribed beyond the predefined distance from the apparent cortical-CSF boundary were rejected, because they were believed to be likely to contain a substantial volume of subcortical white matter. Although the greater visual conspicuity of the GM-white matter junction in areas of apparently abnormal cortex rendered this procedure less critical, the same prior knowledge-based constraint was used to check the ROI prescription on abnormal-appearing images to avoid a systematic bias. A similar constraint was used to decrease the influence of partial volume averaging of CSF by eliminating boundary voxels at the GM-CSF

junction that were likely to contain a significant percentage of CSF. This algorithm was designed to produce cortical ROIs that systematically undersampled the GM of each gyrus to reduce as far as possible the inclusion of adjacent WM and CSF. The defined ROIs were transferred automatically to the ADC maps by the software program for calculation of ADC.

ROIs were selected from the precentral gyri (PMC) and superior frontal gyri (SFG) of the frontal lobes, the postcentral gyri (PSC) and supramarginal gyri (SMG) of the temporal lobes in both hemispheres on every scan. ROI were also selected in thalamus, putamen, and head of caudate nucleus in each patient. ROI measurements of the corresponding anatomic structures from both left and right hemispheres were averaged, and a representative ADC value was obtained for each anatomic region.

To quantify the severity of prion-induced ADC reduction in the normal-appearing Rolandic cortex ROI compared with the ROI selected within the qualitatively abnormal appearing areas of the frontal and parietal lobes, ADC ratios (rADC) were calculated. For example, the ratio of mean ADC of the frontal lobe PMC ROI to the mean ADC of the frontal lobe SFG ROI within the same hemisphere of the same patient was calculated using the formula:  $rADC_{PMC} = ADC_{PMC}/ADC_{SFG}$ . Likewise, the ratio of mean ADC of the parietal lobe PSC ROI to the mean ADC of SMG ROI defined as  $rADC_{PSC} = ADC_{PSC}/ADC_{SMG}$ . If the PMC or PSC were relatively spared, the  $rADC_{PMC}$  or  $rADC_{PSC}$  in patients with CJD would be expected to be significantly greater than the respective  $rADC_{PMC}$  or  $rADC_{PSC}$  ratios in control patients because the ADC of the affected ROI (SFG and SMG) in the denominator would be significantly decreased relative to control and the ADC of the spared ROI (PMC and PSC) in the numerator would be relatively unchanged.

To allow comparison of the cortical rADC with characteristic CJD-related rADC changes in the deep nuclei, the relative ADC of thalamus, putamen, and head of caudate nucleus were also calculated using an average of the frontal and parietal lobe ROI as an arbitrary reference:  $rADC_{ROI} = ADC_{ROI}/ADC_{ref}$  in which  $ADC_{ref}$  was the average of ADC values in SFG and SMG. If the ADC of the deep nuclei ROI were relatively more severely affected than the cortical ROI, then the  $rADC_{caudate}$ ,  $rADC_{putamen}$ , and  $rADC_{thalamus}$  in CJD patients would be expected to decrease relative to the respective control patient rADC ratios because the ADC of the deep nuclei in the numerator would decrease more than the ADC of the neocortex in the denominator.

### Statistical Analysis

The overall difference in each cortical ADC and rADC between the CJD group and control group was analyzed individually by use of the unpaired 2-tailed Student *t* test. A *P* value of 0.05 or smaller was regarded as statistically significant.

### Results

Figure 1A shows the ROI in head of caudate nucleus, putamen, and thalamus on T2-weighted images and the corresponding epiDWI and ADC maps. The SMG ROIs of the same subject are shown in Fig 1B, and PMC, PSC, and SFG are shown in Fig 1C. Bilateral epiDWI signal intensity abnormality was observed in both frontal and parietal lobes (Fig 1B, -C), and corresponding reduction in ADC values was confirmed in the same areas on ADC maps. On the other hand, the PMC and PSC appear normal on epiDWI, but hypointensity suggestive of reduced ADC is seen in the PMC and PSC on ADC maps.

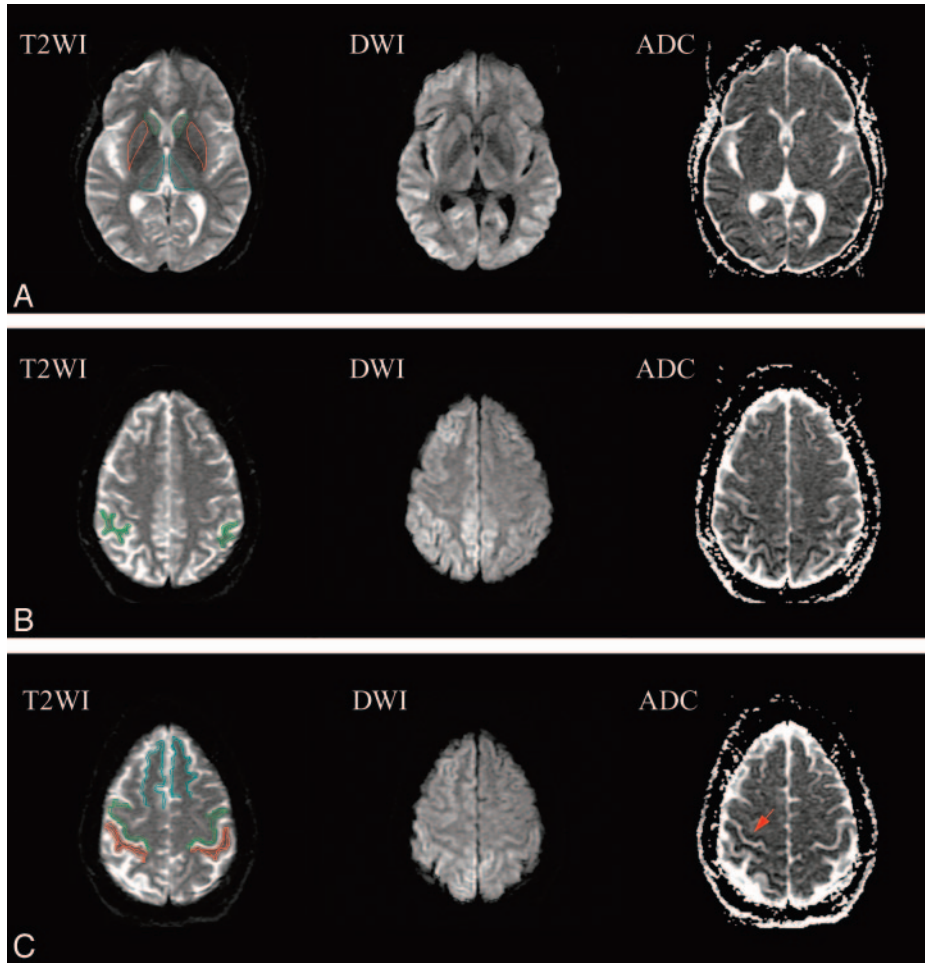


**Fig 1.** ROI in head of caudate nucleus (green), putamen (red), thalamus (cyan) (A), supramarginal gyri (SMG) (B), precentral gyri (PMC) (green), postcentral gyri (PSC) (red), and superior frontal gyri (SFG) (cyan) (C) on EPI B0 T2-weighted images (T2WI), and the corresponding diffusion-weighted images (DWI) and apparent diffusion coefficient maps (ADC). Bilateral abnormal hyperintensity can be observed on DWI with corresponding decreased intensity on ADC maps in thalamus (A) frontal lobes (B), and parietal lobes (C). Characteristic sparing of the PMC and PSC are seen in best in C, where these areas of Rolandic cortex appear normal. Hypointensity can be seen in the right Rolandic cortex on the ADC maps (arrow).

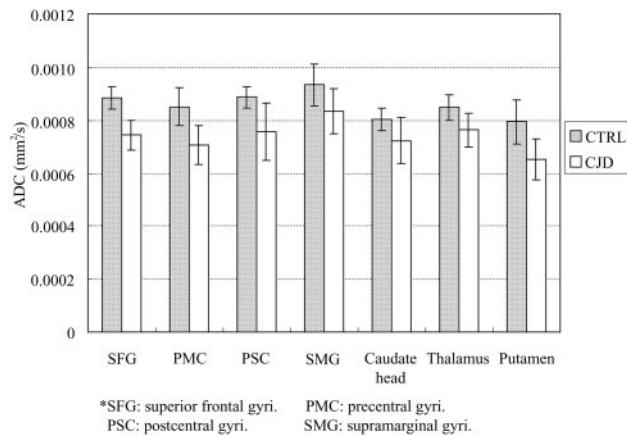


**Fig 2.** ADCs measured in gray matter ROI in patients with CJD (white bars) are significantly lower (14% on average) than ADCs in the corresponding ROI of control patients (shaded bars) in all areas including both commonly affected areas of the frontal lobes (SFG) and parietal lobes (SMG) and typically spared frontal (PMC) and parietal (PSC) Rolandic cortex (individual ROI  $P$  value, 0.001–0.05).

The ADC values measured from different ROIs of both patients with CJD and control subjects are shown in Fig 2. Patients with CJD have statistically lower ADC values than control patients in all areas of neocortical and deep GM sampled ( $P \leq 0.05$ ).

Control patients had an ADC range from  $793 \pm 82$  to  $933 \pm 80$  ( $10^{-6} \text{ mm}^2/\text{s}$ ); patients with CJD had an ADC range from  $650 \pm 77$  to  $833 \pm 86$  ( $10^{-6} \text{ mm}^2/\text{s}$ ). The trend toward decreased ADC in caudate nucleus, putamen, and thalamus correlates well with previously published reports.<sup>9</sup> Unprocessed epiDWI signal intensities were significantly lower in PMC than SFG and PSC than SMG ( $P < 0.0005$ ), in both CJD and control cases, consistent with the reported qualitative observation of “Rolandic sparing.” It is noteworthy that the ratios of PMC/SFG and PSC/SMG epiDWI signal intensities are 0.92 for the CJD group and 0.94 for control group, which are not significantly different between CJD and control cases ( $P > 0.1$ ), confirming that the Rolandic cortex is darker in appearance on epiDWI in both CJD and control patients. We have also observed this in healthy volunteers. As shown in Fig 3, the rADC ratios of PMC/SFG ROI and PSC/SMG ROI did not differ significantly in any ROI between the CJD or control group ( $P > 0.25$ ). This similarity between rADC in the CJD and control groups rejects the hypothesis of physiologic sparing of Rolandic cortex in early CJD.

## Discussion

Recent reports have established high diagnostic accuracy for epiDWI in CJD and described a characteristic distribution of

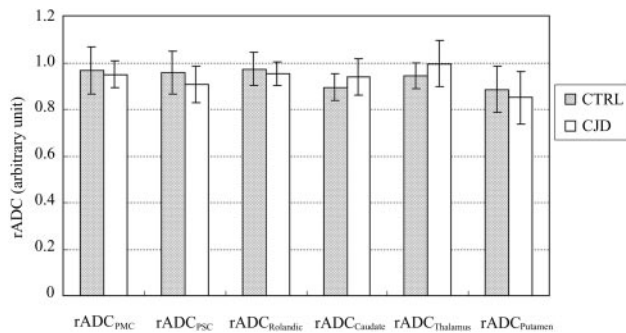


**Fig 3.** rADC ratios between frontal (PMC) and parietal (PSC) Rolandic cortex ROI and commonly affected adjacent frontal (SFG) and parietal (SMG) lobe neocortical ROI in patients with CJD (white bars) do not differ significantly from the equivalent rADC ratios in control patients (shaded bars), confirming that gray matter diffusivity is abnormal to a similar degree in Rolandic cortex and other cortical areas in early CJD, despite apparent “sparing” of Rolandic cortex on DWI (Fig 1C). Likewise, rADC ratios in the deep nuclei do not differ between patients with CJD and control patients, suggesting that the degree of involvement of the caudate, putamen, and thalamus is similar to that of neocortex (individual *P* value range: 0.25–0.70).

abnormality in cortical and deep GM.<sup>5,10,11</sup> One large series established that the appearance of normal signal intensity on epiDWI within primary motor and sensory cortices despite prominent signal intensity abnormality elsewhere in the adjacent frontal and parietal lobes is a characteristic component of this distribution of abnormality, raising the question of why these cytoarchitecturally distinct areas of neocortex should appear to be spared by systemic prion disease. Our quantitative ADC analysis was designed to determine whether this is due to true physiologic sparing of Rolandic cortex or, alternatively, to decreased conspicuity of a global abnormality related to underlying differences between the baseline epiDWI signal intensity in these areas.

Analysis of ADC in the deep nuclei validated our image postprocessing and quantitation method. Although the ADC values measured in caudate nucleus, putamen, and thalamus in our study were somewhat higher than those previously reported, which may result from differences in ROI sizes and degrees of partial volume averaging of adjacent WM and CSF, the trend toward decreased ADC in these areas compared with healthy normal control subjects correlates well with the previously published results.<sup>9</sup> In addition, our quantitative analysis revealed ADC abnormality in areas of the thalamic pulvinar and mediodorsal nucleus of patients with CJD in which no epiDWI abnormality was found by visual inspection. This is also consistent with previous literature demonstrating involvement of these areas in sCJD and suggests that the prevalence of such involvement in sCJD may be higher than the 7% suggested by studies based on epiDWI data.<sup>5,12</sup>

The observed statistical similarity between the rADC of CJD and control groups rejects the null hypothesis of physiologic sparing and indicates instead that the CJD-related reduction in cortical water diffusivity is a global phenomenon, involving the Rolandic cortex to a degree similar to that of other neocortical regions. In other words, the ADC analysis provides quantitative evidence that the sensorimotor cortex is involved early in CJD to a degree similar to that of other areas of the frontal and parietal lobes, as would be expected from the protean nature of the disease. The similarity of PMC/SFG and PSC/SMG epiDWI signal intensity ratios between the CJD and

control cohorts, and the uniform hypointensity of Rolandic cortex epiDWI signal intensity relative to other areas in both patients with CJD and control patients, confirms quantitatively that Rolandic cortex has a different baseline signal intensity on epiDWI compared with other neocortical regions. Thus, the “Rolandic sparing” reported in qualitative epiDWI studies seems likely to be a real phenomenon related to the intrinsic hypointensity of Rolandic cortex relative to other neocortical cytoarchitectonic areas on epiDWI. The aspects of the microstructure of Rolandic cortex that account for this difference in underlying epiDWI signal intensity remain an interesting topic for future investigation. A recent report noting greater phase shift on susceptibility-weighted imaging in cortex adjacent to the central sulcus compared with elsewhere in the brain suggests that local magnetic susceptibility effects may contribute to the hypointensity of these areas on echo-planar imaging sequences including epiDWI.<sup>13</sup> One approach to examining this question would be to use a non-echo-planar DWI technique in addition to epiDWI in a number of these patients.

Weaknesses of this study include the manual ROI selection procedure, which may lower the reproducibility of the quantitative measurements. The adaptation and development of atlas-based automated registration and segmentation techniques to epiDWI GM segmentation is under way in our group to address this limitation in future investigations. In addition, the large voxel size of the 2D epiDWI images in our study raises the possibility that the partial volume-averaging effects could affect the measured ADC values. Partial volume averaging of CSF, which has much higher ADC than GM, would be expected to increase the measured ADC in GM.<sup>14</sup> Partial volume averaging of subcortical WM, which has a lower ADC than GM, would be expected to reduce the measured GM ADC values.<sup>15</sup> To decrease the potential effect of partial volume averaging, we used prior anatomic knowledge to exclude from the ROI boundary voxels that were likely to contain a mixture of CSF or WM with GM. This results in smaller but presumably more homogeneous GM ROI. In addition, the rADC ratio analysis described above should negate any systematic bias introduced by partial volume averaging. For future quantitative studies of cortical diffusivity, higher spatial resolution DWI can be used to differentiate CSF and GM and decrease partial volume effects, or CSF contamination can be eliminated completely using a FLAIR DWI technique.<sup>16,17</sup> Finally, the lack of “gold standard” pathologic correlation in these patients prevents us from stating with certainty that the areas of cortical and deep GM reduced water diffusivity seen early in CJD represent true spongiform degeneration from direct prion infection, though published autopsy data suggest that this is true late in the course of the disease. Given the near impossibility of performing the direct pathologic correlation required to resolve this issue in early CJD, we have chosen to use the somewhat broader term “prion-related injury,” rather than “spongiform degeneration.”

## Conclusion

Quantitative ADC measurements demonstrate abnormal water diffusivity in the primary sensorimotor Rolandic cortex of patients with CJD early in the course of disease, despite the normal appearance of these areas on visual inspection of

epiDWI. The decrease in Rolandic cortex ADC in patients with CJD relative to control patients is similar in magnitude to the decrease in ADC elsewhere in neocortex and in the deep GM. This is consistent with the protean nature of prion disease and suggests that prion-related GM injury affects Rolandic cortex to a similar degree as other areas of neocortex in early CJD. The previously reported “sparing” of these areas on visual inspection of epiDWI seems to represent masking of the abnormally reduced water diffusivity by some intrinsic attribute of the microstructure, possibly the observed baseline hypointensity of these areas on epiDWI. Thus, observation of reduced diffusivity on ADC maps in Rolandic cortex should not be felt to argue against the diagnosis of CJD in the face of a neurologic and MR imaging presentation otherwise suggestive of CJD.

## References

1. Prusiner SB. Molecular biology of prions causing infectious and genetic encephalopathies of humans as well as scrapie of sheep and BSE of cattle. *Dev Biol Stand* 1991;75:55–74
2. Prusiner SB. Prions. *Proc Natl Acad Sci U S A* 1998;95:13363–83.
3. Mittal S, Farmer P, Kalina P, et al. Correlation of diffusion-weighted magnetic resonance imaging with neuropathology in Creutzfeldt-Jakob disease. *Arch Neurol* 2002;59:128–34
4. Murata T, Shiga Y, Higano S, et al. Conspicuity and evolution of lesions in Creutzfeldt-Jakob disease at diffusion-weighted imaging. *AJNR Am J Neuroradiol* 2002;23:1164–72
5. Schroter A, Zerr I, Henkel K, et al. Magnetic resonance imaging in the clinical diagnosis of Creutzfeldt-Jakob disease. *Arch Neurol* 2000;57:1751–57
6. Young GS, Geschwind MD, Fischbein NJ, et al. Diffusion-weighted and fluid-attenuated inversion recovery imaging in Creutzfeldt-Jakob disease: high sensitivity and specificity for diagnosis. *AJNR Am J Neuroradiol* 2005;26:1551–62
7. Russmann H, Vingerhoets F, Miklossy J, et al. Sporadic Creutzfeldt-Jakob disease: a comparison of pathological findings and diffusion weighted imaging. *J Neurol* 2005;252:338–42
8. Stejskal EO, Tanner JE. Spin diffusion measurements: spin echoes in the presence of a time-dependent field gradient. *J Chem Phys* 1965;42:288–92
9. Tschampa HJ, Murtz P, Flacke S, et al. Thalamic involvement in sporadic Creutzfeldt-Jakob disease: a diffusion-weighted MR imaging study. *AJNR Am J Neuroradiol* 2003;24:908–15
10. Bahn MM, Parchi P. Abnormal diffusion-weighted magnetic resonance images in Creutzfeldt-Jakob disease. *Arch Neurol* 1999;56:577–83
11. Ukisu R, Kushihashi T, Kitanosono T, et al. Serial diffusion-weighted MRI of Creutzfeldt-Jakob disease. *AJR Am J Roentgenol* 2005;184:560–66
12. Martindale J, Geschwind MD, De Armond S, et al. Sporadic Creutzfeldt-Jakob disease mimicking variant Creutzfeldt-Jakob disease. *Arch Neurol* 2003;60:767–70
13. Haacke EM, Cheng NY, House MJ, et al. Imaging iron stores in the brain using magnetic resonance imaging. *Magn Reson Imaging* 2005;23:1–25
14. Latour LL, Warach S. Cerebral spinal fluid contamination of the measurement of the apparent diffusion coefficient of water in acute stroke. *Magn Reson Med* 2002;48:478–86
15. Helenius J, Soinnie L, Perkio J, et al. Diffusion-weighted MR imaging in normal human brains in various age groups. *AJNR Am J Neuroradiol* 2002;23:194–99
16. Kwong KK, McKinstry RC, Chien D, et al. CSF-suppressed quantitative single-shot diffusion imaging. *Magn Reson Med* 1991;21:157–63
17. Papadakis NG, Martin KM, Mustafa MH, et al. Study of the effect of CSF suppression on white matter diffusion anisotropy mapping of healthy human brain. *Magn Reson Med* 2002;48:394–98